HAL
open science

# Sandwich composites impact and indentation behaviour study

Belkacem Hachemane, Redouane Zitoune, Boudjema Bezzazi, Christophe Bouvet

## To cite this version:

Belkacem Hachemane, Redouane Zitoune, Boudjema Bezzazi, Christophe Bouvet. Sandwich composites impact and indentation behaviour study. Composites Part B: Engineering, 2013, vol. 51, pp. 1-10. 10.1016/j.compositesb.2013.02.014 . hal-00859791

## HAL Id: hal-00859791
## https://hal.science/hal-00859791v1

Submitted on 9 Sep 2013

**HAL** is a multi-disciplinary open access archive for the deposit and dissemination of scientific research documents, whether they are published or not. The documents may come from teaching and research institutions in France or abroad, or from public or private research centers.

L'archive ouverte pluridisciplinaire **HAL**, est destinée au dépôt et à la diffusion de documents scientifiques de niveau recherche, publiés ou non, émanant des établissements d'enseignement et de recherche français ou étrangers, des laboratoires publics ou privés.

Open Archive Toulouse Archive Ouverte (OATAO)
OATAO is an open access repository that collects the work of Toulouse researchers and makes it freely available over the web where possible.

This is an author-deposited version published in: http://oatao.univ-toulouse.fr/
Eprints ID: 9327

**To link to this article**: DOI: 10.1016/j.compositesb.2013.02.014
URL: http://dx.doi.org/10.1016/j.compositesb.2013.02.014

**To cite this version**: Hachemane, Belkacem and Zitoune, Redouane and Bezzazi, Boudjema and Bouvet, Christophe *Sandwich composites impact and indentation behaviour study.* (2013) Composites Part B: Engineering, vol. 51. pp. 1-10. ISSN 1359-8368

Any correspondence concerning this service should be sent to the repository administrator: staff-oatao@inp-toulouse.fr

# Sandwich composites impact and indentation behaviour study

B. Hachemane [a,*], R. Zitoune [b], B. Bezzazi [a], C. Bouvet [c]

[a] Boumerdès University, FSI, Materials, Process & Environment Research Unit, 1 av. de l'indépendance, 35000 Boumerdès, Algeria
[b] Toulouse University, UPS, Clement Ader Institute, 133 av. de Rangueil, F-31077 Toulouse, France
[c] Toulouse University, ISAE, Clement Ader Institute, 10 av. Edouard Belin, F-31077 Toulouse, France

ARTICLE INFO

*Keywords:*
B. Impact behaviour
C. Damage mechanics
D. Mechanical testing
E. Lay-up
Sandwich materials

ABSTRACT

In order to better exploit the natural cork available in Algeria, an experimental characterisation of a jute/epoxy–cork sandwich material to impact and indentation was undertaken. The aim of this work is to evaluate the impact energy and cork density influence over the sandwich plate damage behaviours by instrumented static and dynamic tests. The results show that the onset damage force, the maximum force and the damage size are influenced by the cork density and the impact energy. The sandwich material, with the heavy agglomerated cork having a density of 310 kg/m$^3$ is characterised by a weaker energy dissipation capacity, by about 3.72% for impact test and 3.29% for indentation one, than the sandwich with lighter cork (160 kg/m$^3$). This difference is an infusion process consequence. The infiltrated resin into the agglomerated cork pores changes the material local rigidity. Also, under impact loading the sandwich laminates dissipate 11% more energy than with the quasi-static indentation test.

## 1. Introduction

In the composites reinforcement, the natural fibres use is growing, primarily because of environmental and economics concerns. Natural fibres mostly used are straw, flax, hemp and jute. Compared to hemp fibre, jute has the advantage of being easy to weave [1]. Although the mechanical performance of natural fibre composites offer new perspectives for the design of structures (low density, acceptable mechanical properties), the variability of their behaviour of these materials make them difficult to use [1,2]. In addition, the reproducibility of their properties is not easy to ensure because of their dependence on various parameters such as the grain plant origins, the soil type on which they were planted, weather condition and the maturation of the plants, etc. Several studies have shown that these materials are sensitive to moisture and heat [3]. When these materials are heated at different temperature levels, there was a notable decrease in their tensile, flexural and shock strengths. For example, the tensile tests carried out on a fabric jute at different temperatures showed a drop in the tensile strength of 43% when it is heated to 180 °C [1]. Moreover, jute is a hydrophobic material and moisture absorption alters the dimensional and mechanical characteristics of jute fibres laminate [4–7]. The results reported by Karmaker [4] showed that after one day of water immersion, the thickness of a jute/polypropylene laminate, with 35% fibre of volume ratio, increases by 0.75%. Also, the Rahman et al. work [6] showed that the jute/PP composite mass increases by 1.2% after 2 h immersion in hot distilled water. Therefore, Akil et al. [5] experimental tests indicate that the jute/polyester bending strength decreases by 30% after one day in distilled water immersion, whereas Khan et al. [7] reported that jute fibres absorb up to 19% water after one minute of immersion in 25 °C deionised water.

The jute/PP composite gave better tensile and flexural strength compared to flax/PP and abaca/PP laminates (between 10% and 20% higher) [8], whereas mat hemp/epoxy showed 8.5% more tensile strength and 14% better elasticity modulus than the woven jute/epoxy laminates [9], unlike the bending strength which was 5.8% less. Jute/epoxy composites were broken by fibres tearing followed by matrix cracking [9]. This same observation was made by Ray et al. [10] for jute/vinylester laminate and O'Dell [11] for jute/unsaturated polyester composite. As for the most common jute/polyester damage modes are matrix cracking and fibres breaking [4]. A tensile fracture surface electron microscopy analysis of jute/PP material [12] and jute/L-polylactide composite [13] shows that these materials behaviour is brittle.

The mechanical properties of the jute/epoxy skin are very low compared to the carbon/epoxy skin or the glass/epoxy skin. However this material has good properties compared to the natural fibres like flax, abaca and hemp [8,9].

Few works have focused on the analysis of jute fibre reinforced laminates behaviour subjected to impact loading by falling weight. In one of these researches, an experimental study was conducted in order to show the influence of hybridization of glass fibres (jute–glass hybrid composites) on low velocity impact response, damage resistance and damage tolerance capability of composites made by

* Corresponding author. Tel.: +213 554234495; fax: +213 24913866.
*E-mail address:* bhachemane@yahoo.fr (B. Hachemane).

isothalic polyester reinforced by a woven jute fabric [14]. The results show that the jute composites have better energy absorption capacity compared to jute–glass hybrid laminates. However, the hybrid laminate with 16% glass fibre weight is the most optimum combination of jute and glass fibre with minimum deflection, maximum peak load, and better damage tolerance, than the hybrid laminates with 25.2% and 8.2% glass fibre weight fraction.

Using the acoustic emission technique and thermo-elastic stress analysis, cyclic post-impact three-point bending tests were carried out on plain woven jute fabric/polyester plates [15]. This research showed that damage in natural fibre reinforced laminates progresses as far as the defects present in the laminate until they reach a critical energy that allows them to grow. On impact by foreign object, the composite jute/vinylester absorbs more impact energy by deformation (permanent indentation) than by delamination [16]. As for the impact energy increases, it has a limited affect on the residual strength bending of jute/polyester. A decrease of 38.5% was observed after an impact of 20 J [15]. However, at higher impact energies, the damaged surface area may be very largely increased (an increase of 845% was noted when the woven jute/polyester composite impact energy is increased from 5 to 15 J) [17]. The damage along the specimen thickness is conical shaped called "inverted pine tree".

The agglomerated cork is an ideal core material for composite sandwich constituting light structures, such as those used in aerospace applications. Static bending and shear tests have been carried out on carbon/epoxy-cork sandwich samples [18]. The test results show that the cork performance depends mainly on density and grain size. Increasing the cork density from 137 to 270 kg/m$^3$, its shear strength was found also increase by 242%. Different agglomerated cork used had a similar failure mode: mode "I" crack initiation at the maximum load, crack propagation and intergranular final fracture. During the cork core sandwich bending, the maximum force, shear strength and modulus increase with grain size decreasing synonym of cork density growing.

An epoxy resin incursion between the cork grains, in jute/epoxy skins and cork core sandwich laminates prepared by infusion process, increases the shear stiffness by 1.8 times for cork density of 270 kg/m$^3$ and 2.8 times for 190 kg/m$^3$ [19]. At high temperatures, both corks are losing a large mass in the early hours. This loss is not identical for the different agglomerated cork, with or without epoxy resin incursion (5% for cork 190 kg/m$^3$ and 4.5% for cork 270 kg/m$^3$, after heating at 100 °C during 10 h). The cork density and the epoxy resin incursion influence its ability to absorb water. The resin presence in the cork 270 kg/m$^3$ increases its water absorption capacity by 26%.

The impact of sandwich with cork core and carbon/epoxy skins has also received little attention. A comparison between the mechanical behaviour during impact of sandwich plates with foam core and those with cork core has shown that the last ones have a maximum impact force larger than the first panels. The minimum difference observed is about 25%. In addition, the sandwich laminates with cork core have a more important capacity to absorb the impact energy with low depth damage [20]. Finally, recent works show the thermal protection influence on impacted damaged composites structures used for launcher's fairing. Experimental tests were conducted on cork shielded and unshielded panels [21]. The results showed that for a Carbone/epoxy unidirectional laminate T300/914, the delamination onset energy is about 3 times greater when the cork thickness is 3.5 mm and about 7 times greater when the thickness is 6.5 mm.

For better exploitation of the available resources in Algeria and with the economic and environmental benefits that this country holds, this research might be used to lighten the building construction by replacing existing solutions (insulation bricks, plaster, siporex, etc.) by sandwich panels made from jute/epoxy skins and agglomerated cork core manufactured by the infusion process. Nevertheless, sandwich plates can be subjected to accidental damage such as a falling object (e.g. hammer, screwdriver, etc.), and therefore it is necessary to characterise this material during the low energy dynamic impact loading and compare results with quasi-static indentation loads.

With the mentioned background, this work deals with the mechanical behaviour of sandwich panels made of jute/epoxy skins and cork core under low energy impact and quasi-static indentation. The main goal is to carry out an experimental study in order to determine the influence of impact energy and cork density, by means of the force–displacement curves and the damage size, and propose a jute/epoxy-cork composite sandwich damage chronology.

## 2. Experimental procedure

### 2.1. Material

The employed material is a sandwich composed of jute–epoxy skins and cork core, manufactured by one-shot infusion method. In this case, the jute woven skins and the cork core are infused in only one step, as shown in Fig. 1. The skins are laid-up with a $[0°]_s$ stacking sequence. The skin mechanical properties are given in Table 1 [1]. Three cork densities are studied with the following values 160, 270 and 310 kg/m$^3$. These values correspond to a 4–16, 3–5 and 1–2 mm granulate size respectively. The employed epoxy resin is referenced as LY5052, associated to its HY5052 hardener. When the infusion is completed, the obtained sandwich is polymerised in a woven at 80 °C during 12 h. The Table 2 gives the sandwich specimen's final dimension manufactured with the mentioned materials (see Fig. 2).

### 2.2. Impact tests

The experimental equipment used for the impact tests is illustrated in Fig. 3. It is mainly composed by a guide column supporting a Kistler force sensor equipped with an impactor. Two laser sensors and an oscilloscope are the measuring devices. A rigid table with a 125 × 75 mm$^2$ window holding system, where the sandwich plates are held to complete the parts of the equipment.

The impactor is composed by a 2 kg free falling main block coupled with a 10 KN force sensor and a 12.7 mm diameter hemispherical tip. The first laser sensor allows calculating the starting contact velocity; meanwhile the second gives the displacement

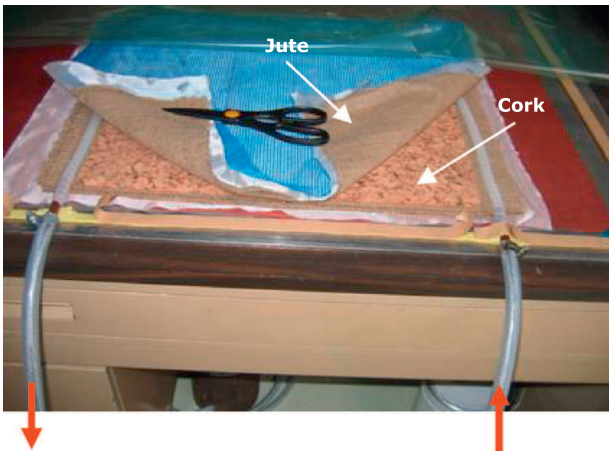


**Fig. 1.** Manufacturing process by infusion of sandwich panels.

**Table 1**
Mean mechanical properties of composite jute/epoxy [1].

| Density (kg/m$^3$) | $E_t$ (GPa) | $E_f$ (GPa) | $G$ (GPa) | $\nu_{lt}$ | $\nu_{tl}$ | $\sigma_{tR}$ (MPa) | $\sigma_{fR}$ (MPa) | $\tau_R$ (MPa) |
|---|---|---|---|---|---|---|---|---|
| 1165 ± 0.01 | 4.5 ± 0.6 | 3.2 ± 0.2 | 1.45 | 0.24 | 0.27 | 38 ± 6 | 80 ± 8 | 23 |

**Table 2**
Mean geometrical parameters of sandwich specimens.

| Sandwich reference | Cork density (kg/m$^3$) | $b$ (mm) | $e_a$ (mm) | $h$ (mm) | $L$ (mm) | $e_s$ (mm) |
|---|---|---|---|---|---|---|
| SD 160 | 160 | 100.22 ± 0.4 | 10.48 ± 0.8 | 13.32 ± 0.5 | 150 | 1.42 ± 0.15 |
| SD 270 | 270 | 100.5 ± 0.21 | 12.04 ± 0.67 | 14.86 ± 0.49 | // | 1.41 ± 0.09 |
| SD 310 | 310 | 100.37 ± 0.42 | 11.13 ± 0.37 | 14.61 ± 0.17 | // | 1.74 ± 0.1 |

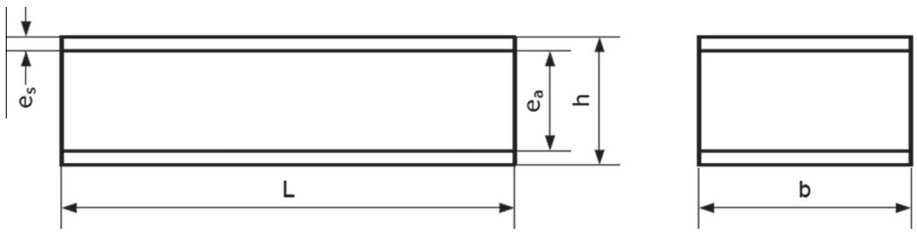


**Fig. 2.** Geometry of sandwich panel.

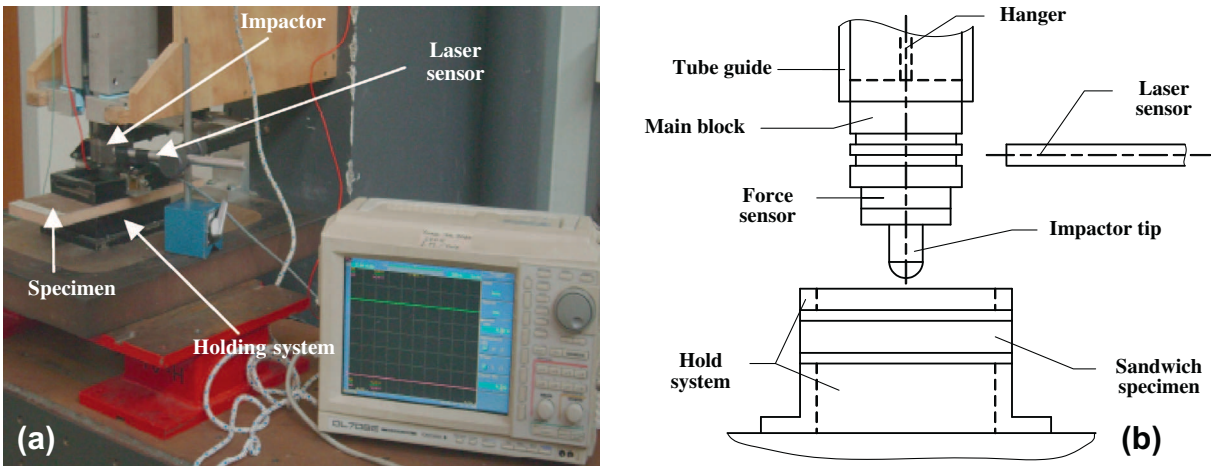


**Fig. 3.** Impact equipment. (a) Experimental device with recording system and (b) device scheme.

of the non-impacted side. The sensor's signals are synchronised by the oscilloscope.

The impact force, $F_{impact}$, between the impactor and the specimen is determined from the sensor measured force, $F_{measured}$, by the Eq. (1):

$$F_{impact} = \frac{m_{impactor}}{m_{impactor} - m_{tip}} F_{measured} \tag{1}$$

where $m_{impactor}$ and $m_{tip}$ are the impactor total mass (2.056 kg) and the hemispherical tip mass (0.176 kg), respectively.

As a consequence of the absence of a specific standard impact test method for sandwich structures, impact tests were performed following the recommendations of ASTM D7136/D7136M-05, which suggest the Eqs. (2)–(4) for obtaining the main testing results:

$$E_i = \frac{m_{impactor}}{2} V_i^2 \tag{2}$$

$$\delta(t) = \delta_i + V_i\, t + \frac{g}{2}\, t^2 - \int_0^t \left( \int_0^t \frac{F_{impact}\,(t)}{m_{impactor}}\, \mathrm{dt} \right) \mathrm{dt} \tag{3}$$

$$E_p(t) = \frac{m_{impactor}}{2} \left( V_i^2 - V(t)^2 \right) + m_{impactor}\, g\, \delta(t) \tag{4}$$

where $E_i$ is the impact energy (J), $V_i$ is the impact velocity (m/s), g is the acceleration due to gravity (9.81 m/s$^2$), $V(t)$ is the impactor velocity at time $t$ (m/s), $\delta_i$ is the impactor displacement from the reference position at time $t = 0$ (m), $\delta(t)$ is the impactor displacement from the reference position at time $t$ ($m$) and $E_p(t)$ is the sandwich plate energy at time $t$ (J).

### 2.3. Indentation tests

For quasi-static indentation tests, we used a 4206 Instron machine. The machine force sensor (10 KN) provides the force signal applied to the specimen. The indentor is identical to that used in

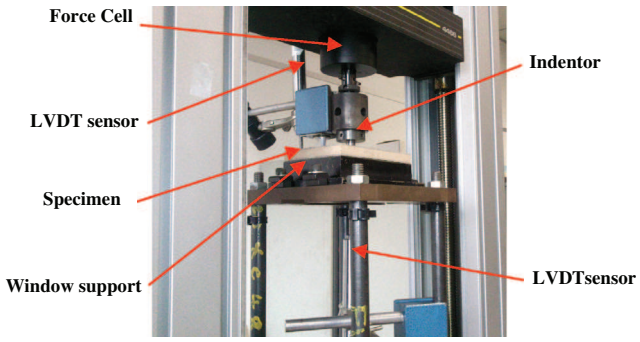


**Fig. 4.** Equipment arrangement for indentation testing.

**Fig. 5.** Three-dimensional measuring machine "MC 1200C".

impact tests. The indentor displacement $s(t)$ is controlled by those of the testing machine crossbar, while loading and unloading test speeds are 2 mm/min. The indentor displacement and the opposite side deflection are measured by two LVDTs installed parallel to the vertical axis (Fig. 4). The displacements are obtained through the respective conversion factors. Among other things, Solatron LVDTs types BS25 were used during testing. The three signals (force and two displacements) are recorded by the data acquisition system Yokogawa DL708.

The machine force sensor signal can be directly used to determinate the force acting on the specimen, $\Delta 1\ V = \Delta 1$ KN while the displacements are obtained by converting the two LVDTs voltage signals:

$$\delta_{st}(t) = 2.5\ \frac{\text{mm}}{\text{V}} * \text{U}_{\text{LVDT1}}(t) \tag{5}$$

$$f_{st} = 2.5\ \frac{\text{mm}}{\text{V}} * \text{U}_{\text{LVDT2}}(t) \tag{6}$$

where $2.5\ \frac{\text{mm}}{\text{V}}$ is the conversion factor. The plate energy is obtained by an identical manner to that used in the dynamic tests:

$$E_p(t) = \int_0^{\delta_{st}(t)} F(t)\, d\delta_{st}(t) = F(t) * \Delta\delta_{st}(\Delta t) + E(t - \Delta t) \tag{7}$$

During the test, the energy reaches a maximum value. However, a residual energy value is recorded at the end of the test which represents the energy dissipated during the specimen damage.

In this study and to verify results repeatability, we repeated only the impact and equivalent indentation tests for 7 and 10 J energies.

After the impact and the quasi-static indentation tests, the permanent indentation depth are measured using a three-dimensional measuring machine "MC 1200C" (Fig. 5). To measure the indentation depth, the machine is equipped with an electronic probe with which we crate plate upper surface referential representing the zero level. Then, the probe scans the damaged zone and gives the indentation depth.

## 3. Results and discussion

### 3.1. Impact tests

The results in Fig. 6 show the evolution of the impact force vs. time for four impact energies, obtained on a SD 310 sandwich plate. It is noticed that for impact energies below 15 J, these curves are not far removed from a sine wave. The impact test performed with energy of 15 J resulted in a damage of the non-impacted skin. From Fig. 6, two critical values can be distinguished, the first one relates the first damage force, and the second one represents the maximum impact force recorded by the force sensor, which are noted as $F_0$ and $F_{max}$, respectively. For a 310 kg/m$^3$ cork density, the first damage force increases with impact energy. This growth is about 40% when the impact energy increases from 5.22 to 9.95 J.

Fig. 7 shows the impact force evolution vs. the displacement calculated from Eq. (3) for a SD 310 sandwich plate. Up to a displacement of about 0.25 mm, dynamic effects due to the plate iner-

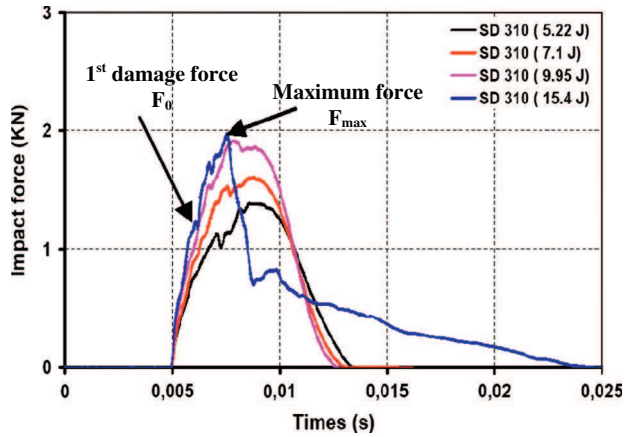


**Fig. 6.** Temporal impact force curves for the SD 310 composite sandwich.

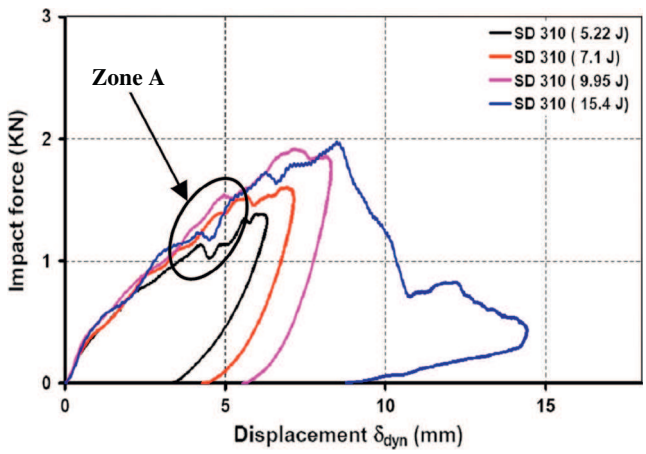


**Fig. 7.** Impact force vs. impactor displacement curves for the SD 310 composite sandwich.

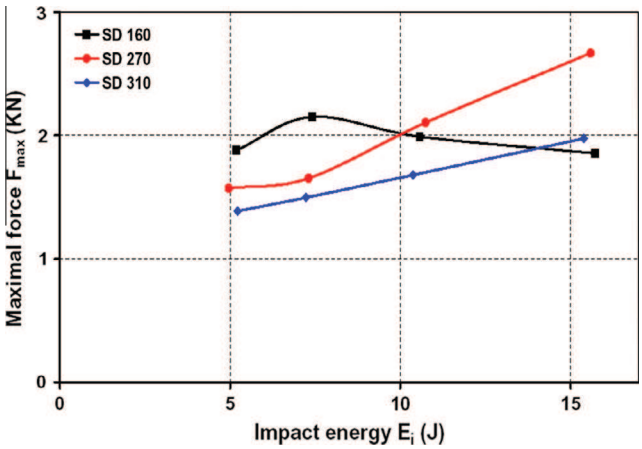


**Fig. 8.** Maximum force $F_{max}$ vs. impact energy.

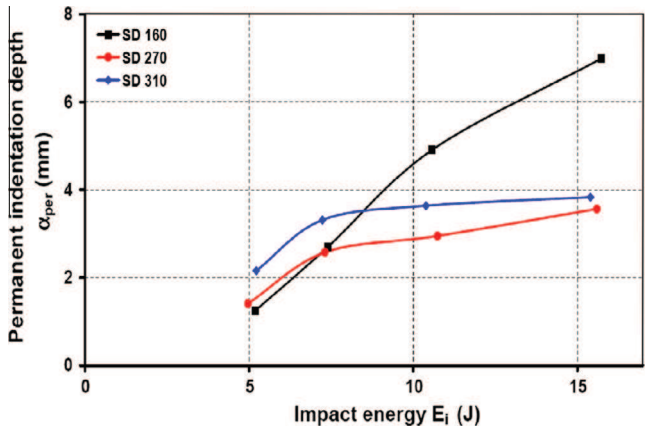


**Fig. 10.** Permanent indentation vs. impact énergies.

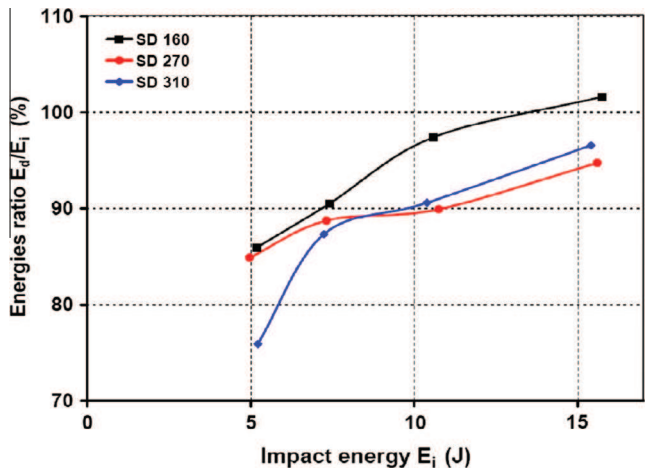


**Fig. 11.** Energies ratio $E_d/E_i$ for the different sandwich materials.

tia can be observed. In the following analysis, they will be neglected. Subsequently, we recorded a linear force evolution (plates bending stiffness being of the order of 0.74 KN/mm) until approximately 0.6 mm displacement where variations begin to appear. They are caused by the specimen's damage onset. A second linear evolution follows with a 0.25 KN/mm slope which is much lower compared to the first one, this means that the plate rigidities decreases. Nevertheless, the force continues to increase despite other minor damage formation. When the maximum displacement is reached, the force begins to decrease steadily to zero.

After the appearance of the first damage, a slight drop in the sandwich plate linear stiffness is registered, noted as zone A (Fig. 7). During a short time, the plate returns to its linear stiffness with the appearance of several oscillations followed by a gradual increase in the force signal. This can be explained on one side by the numerous damages caused by the impactor penetration into the specimen, and on the other hand, by the increment of the cork density due to the compression phase which leads to a compression modulus growth. The compression phenomenon was demonstrated in previous works during quasi-static compression tests on natural cork [22]. Also, during the compression phase, three phenomena corresponding respectively to the elastic bending, the buckling and the crushing of the cell walls are identified. The oscillations observed in Fig. 7 may be related to the buckling phenomenon. Also, it is noticed that the residual displacement for SD 310 sandwich laminates increases with the impact energy; in fact it increases from 3.3 to 5.6 mm when the energy grows from 5.22 to 9.95 J. However, for the SD 160, the residual displacement is more important. In this case, when the impact energy doubles, residual displacement is greater than three times, from 2.32 mm for 5.18 J to 7.84 mm for 10.37 J.

The levels of maximum force recorded by the sensor are strongly influenced by the cork density. As shown in Fig. 8, the

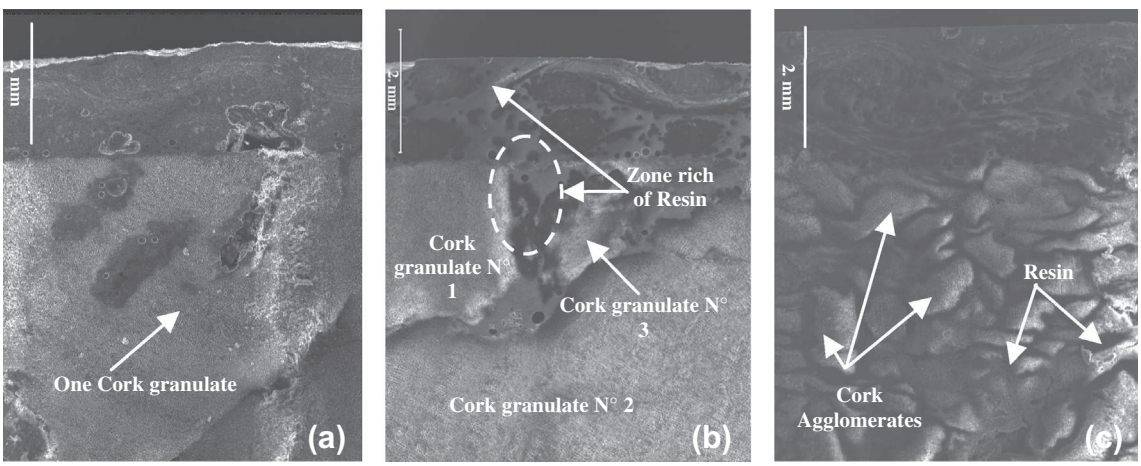


**Fig. 9.** SEM observation of sandwich SD 160 and SD 310. (a) SD 160 with one cork agglomerate, (b) SD 160 with 3 cork agglomerates, and (c) SD 310 with various cork agglomerates.

**Table 3**
Overview of the conducted dynamic tests on the jute–epoxy/cork sandwich specimens.

| Sandwich reference | $E_i$ (J) | $\delta_{dyn\ max}$ (mm) | $F_{dyn\ max}$ (KN) | $\alpha_{per}$ (mm) | $E_d/E_i$ (%) |
|---|---|---|---|---|---|
| SD 160 | 5.18 | 3.73 | 1.88 | 1.24 | 85.93 |
| | 7.41 | 5.64 | 2.15 | 2.7 | 90.51 |
| | 10.57 | 8.68 | 1.99 | 4.91 | 97.39 |
| | 15.73 | 15 | 1.86 | 6.99 | 101.62 |
| SD 270 | 4.97 | 4.72 | 1.57 | 1.41 | 84.89 |
| | 7.31 | 6.98 | 1.65 | 2.57 | 88.58 |
| | 10.74 | 8.18 | 2.1 | 2.95 | 89.74 |
| | 15.59 | 9.07 | 2.67 | 3.56 | 94.75 |
| SD 310 | 5.22 | 6.3 | 1.39 | 2.16 | 75.93 |
| | 7.23 | 8.06 | 1.5 | 3.31 | 87.14 |
| | 10.38 | 9.57 | 1.68 | 3.64 | 90.45 |
| | 15.4 | 14.42 | 1.98 | 3.83 | 96.56 |

maximum force decreases from 1654 to 1497 N when the cork density increases from 270 to 310 kg/m$^3$ for 7 J impact energy. This can be explained by the fact that low cork density increases the grain size which results into a higher porosity. This implies that during the manufacturing of the sandwich plates, the resin infiltrates into the pores increasing the local rigidity of the material, as shown in Fig. 9. However, for the lowest cork density, SD 160, the force distribution recorded as a function of impact energy shows a random distribution. This distribution may be related to the impactor/target local contact area, which can occur either over a cork grain as shown in Fig. 9a, or over a cork-resin interface as illustrated in Fig. 9b, or totally on a rich zone of resin as indicated in Fig. 9b. Concerning the other densities, this observation is not completely true as seen in Fig. 9c. In the latter, the plate consists with a small cork grain sizes. This does not allow a large amount of resin infiltration to the plate inside. By cons, for Fig. 9a and b,

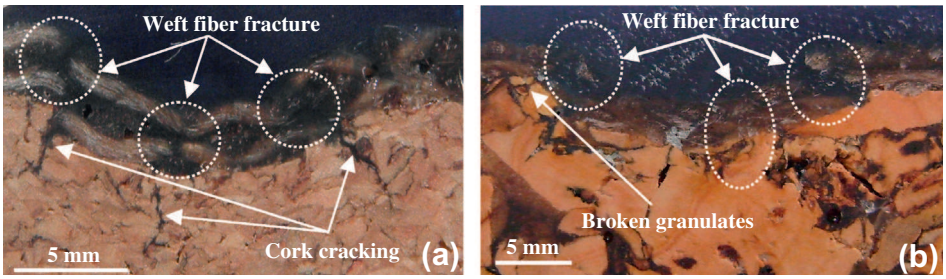


**Fig. 12.** Cross section photographs showing the damage state for two sandwich laminates with 7 J of impact energy. (a) SD 310 sandwich and (b) SD 160 sandwich.

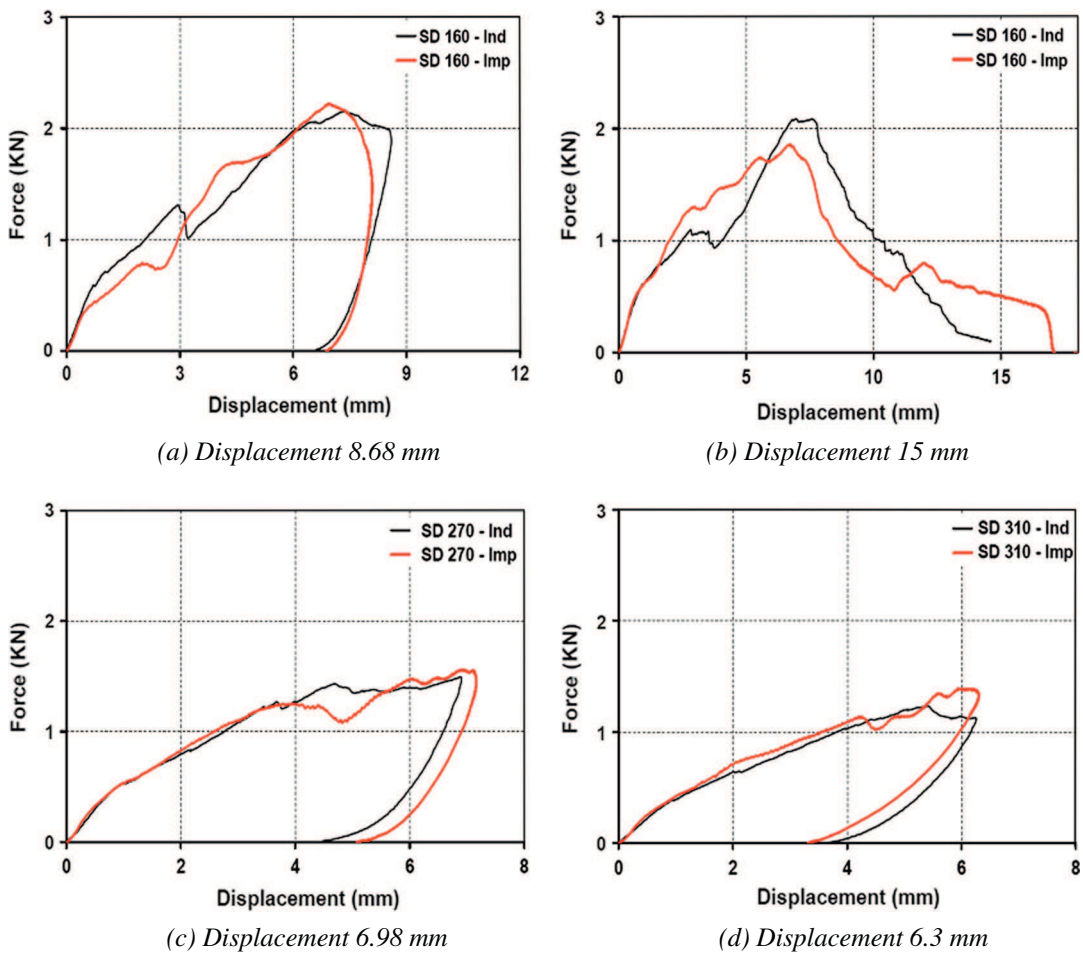


**Fig. 13.** Comparison of the force–indentor displacement curves for the indentation and impact tests on the jute/epoxy-cork sandwich laminates.

the cork have very high grain sizes so impressive pores are filled with resin during the plate manufacture by vacuum infusion.

The plot in Fig. 10 shows the permanent indentation depth $\alpha_{per}$ evolution for the three sandwich materials as a function of the impact energy. When the impact energy rises from 5 to 7 J, a significant increase in permanent indentation depth is recorded for all tested densities. It is also noticed that for the impact energies superior to 7 J, the permanent indentation depth increases slowly for the SD 270 and SD 310 sandwich laminates. However, for the SD 160 sandwich, the permanent indentation depth increases significantly until the total specimen rupture. This difference may be related to the difference of energy dissipated by the three materials as well as to the energy dissipation modes.

The results of Fig. 11 show the cork density and the energy of impact influence on the sandwich dissipated energy-impact ratio $E_d/E_i$. It is observed that an increase in the cork density causes a decrease of the energies ratio. For 5 J impact energy, the cork density transition from 310 to 160 kg/m$^3$ raises the $E_d/E_i$ ratio from 76% to 86%. If the impact energy grows, this trend is still observed but the difference is less important. As it can be seen, the $E_d/E_i$ ratio only raises by 3.2% with 7 J impact energy.

With the less dense cork, the resin quantity which infiltrates the pores is more important. Therefore an increment in the resin quantity results in a change of the material proprieties. In this case, the local stiffness is not the same and thus its ability to absorb energy. Table 3 summarises the main performed impact test results.

The various failure mechanisms that can occur during a sandwich laminates panel's impact are [23]:

- Skin fracture in tension or compression.
- Core fracture in tension or compression.
- Shear failure.
- Skin-core delamination.
- Upper skin local damage under the impactor.

In Fig. 12, it is shown the post-impact damage state of the sandwich panels for 7 J impact energy. The cork damaged areas, for the SD 310 sandwich laminates, are manifested by the presence of cracks between granulate interfaces, as observed in Fig. 12a. However when the density is lower than 310 kg/m$^3$, in addition to interface granulate cracks, cracks through the cork granulates and cork failure by compression are also observed (Fig. 12b). In the case of rovimat/polyester–PVC foam sandwich panels impact (Ei is of the order of 200 J), core damage leads to ±45° transverse shear failure in the foam. This is due to the failure propagation at the core/skin sandwich material interface [23].

Concerning the impacted skins, the observed damage is produced by two loading modes. At the impactor centre, compressive laminate fracture is noticed for all sandwich panels. However, shear damages are detected near the impacted area.

The cork-based sandwich (regardless the type of granulate) presented considerably higher load values than those obtained for other type of high performance core materials. Compared with high performance foams, sandwich components with cork agglomerates have a high energy absorption capacity with minimum damage occurrence, resulting in better crashworthiness properties when impact loading is expected during service [20].

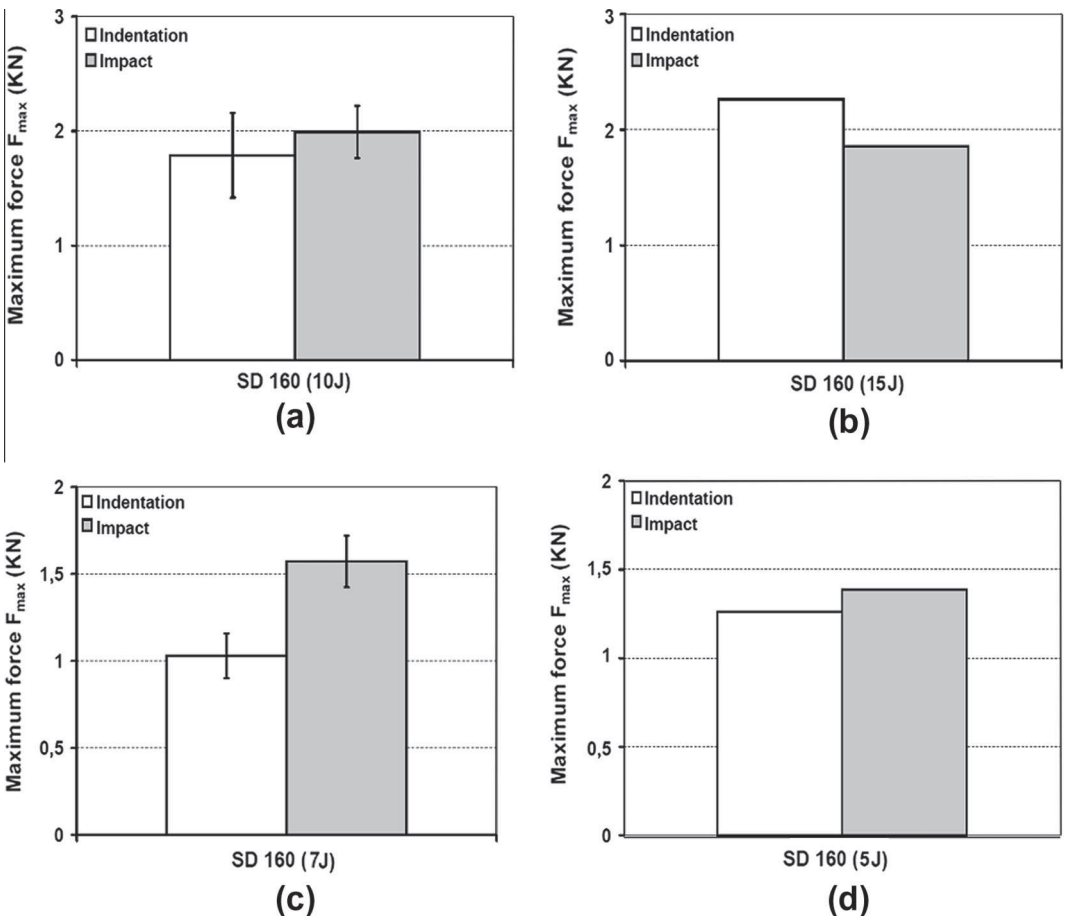


**Fig. 14.** Comparison of dynamic and static tests with respect to the maximal force.

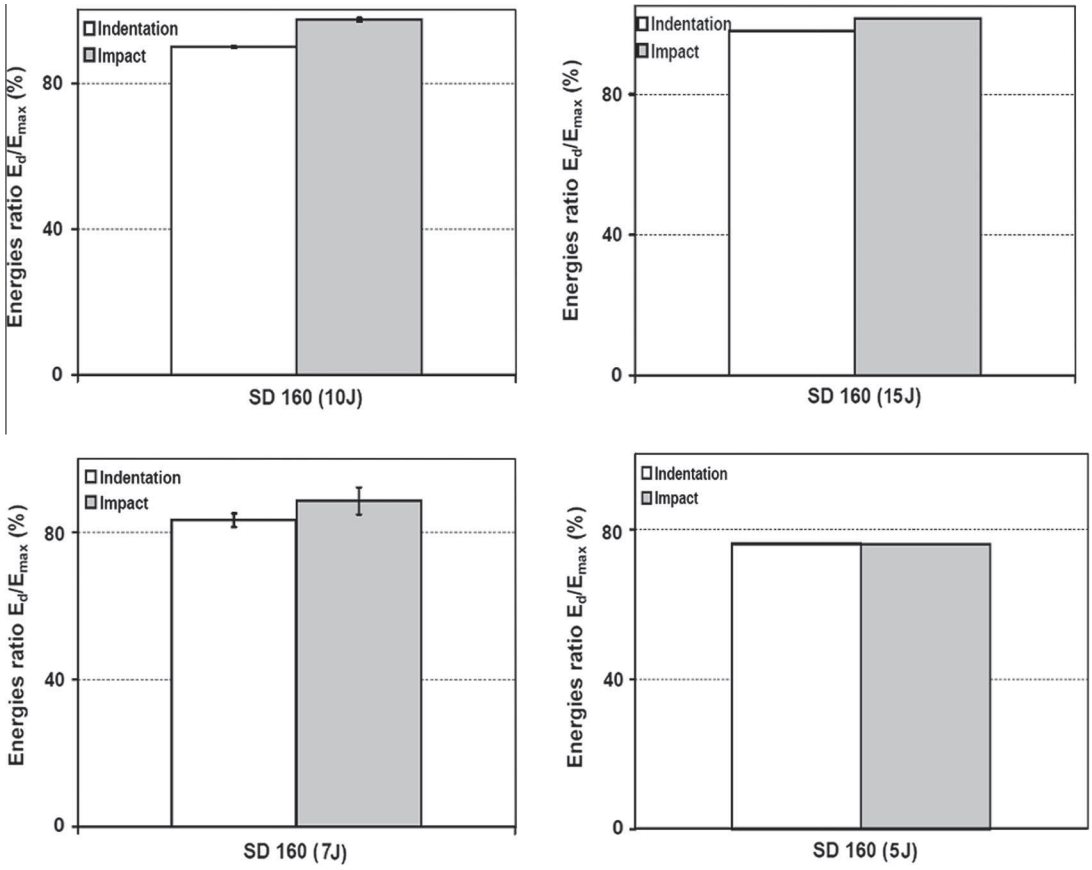


**Fig. 15.** The energies ratio "$E_d/E_{max}$" as function of the maximal energy.

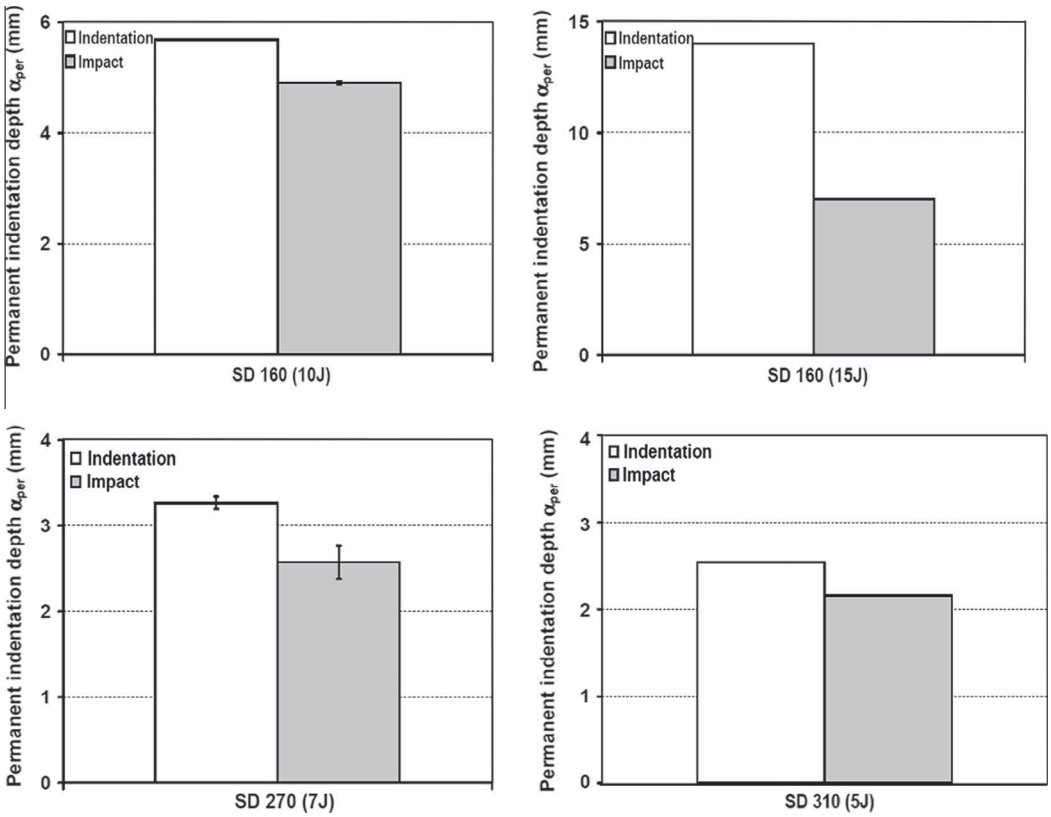


**Fig. 16.** Permanent indentation depth histograms for the jute/epoxy-cork sandwich laminates.

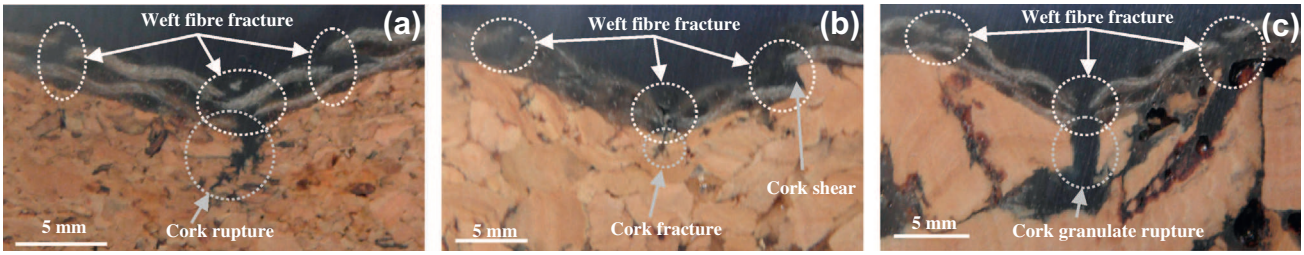


**Fig. 17.** Cross section photographs showing the damage state for three sandwich laminates after indentation tests. (a) SD 310 Sandwich, (b) SD 270 Sandwich, and (c) SD 160 Sandwich.

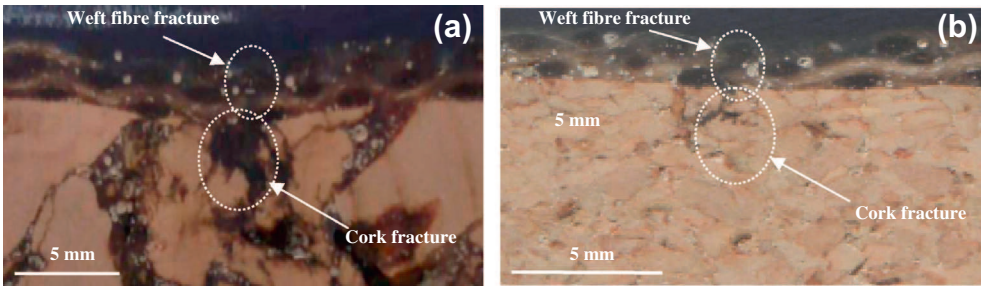


**Fig. 18.** Cross section photographs showing the damage state for two sandwich laminates after first indentation damage. (a) SD 160 Sandwich and (b) SD 310 Sandwich.

### *3.2. Comparison of dynamic and static tests*

The static and dynamic tests have a common parameter, i.e., the maximum indentor displacement. Thus, a good opportunity is given to compare the results of both test types. First, a force–displacement curves comparison is performed for tests with the same maximum displacement (Fig. 13). The curve slopes (specimens bending stiffness $\frac{\partial F}{\partial \delta}$) for the two linear sections are identical for static and dynamic loading. As the load is more stable during indentation tests compared to the impact, the generated forces are better distributed over the plate.

Fig. 14 shows the maximum force evolution for impact and indentation tests. Generally, the maximum force values were greater during the impact tests (about 11.17%, 1.85% and 10.32% for SD 160, SD 270 and SD 310 respectively). In Fig. 14b, the maximum force value for impact test is lower than that of the indentation one. This can be explained, as it has been suggested previously, by the impactor/plate contact area which can occur either over a cork grain (Fig. 9a) or over a cork-resin interface or totally on rich zone of resin (Fig. 9b).

The area under the force–displacement curve until the maximum displacement is the maximum or total tested plate energy:

$$E_{\max}(\delta) = \int_0^{\delta_{\max}} F\, d\delta \tag{8}$$

The greater the area in the indentation hysteresis cycle, the larger the energy dissipated by the plate. This dissipated energy is due to the damage formation in the specimen. A comparison of the "$E_d/E_{\max}$" energies ratio based on the maximum energy is illustrated in Fig. 15. It should be noted that this ratio is generally higher in impact than in indentation tests (between 3.61% and 8.25% for SD 160, and 6.29% for SD 270). This difference may be related to the kinematics deformations, which is faster in the impact tests compared to the indentation ones. During dynamic tests, the effort exerted on a microscopic element increases rapidly that does not leave enough time for the load transfer.

Although the energy dissipation is higher for dynamic tests, the permanent indentation depth "$\alpha_{per}$" is larger during the quasi-static indentation (Fig. 16). The permanent indentations generated by indentation tests are 16% deeper for SD 160, 27% for SD 270, and 17% for SD 310 compared to those of impact tests.

Fig. 17 shows the post-indentation damage on sandwich panels. Sandwich SD 310 cork damage manifests by the intergranular cracks (Fig. 17a). However, when the cork density is less than 310 kg/m$^3$, intergranular cracking is replaced by a cork grain crack (Fig. 17b) or grain rupture (Fig. 17c). Concerning the impacted skin, the observed damages are generated by two loading types: laminate compression fracture in the indentor centre for all the sandwich panels with skin shears on the vicinity of the damaged area.

During the jute/epoxy-cork sandwich material indentation loading, the first damage to appear is upper skin compression cracking (indentation) at the impact zone followed by cork intergranular cracking (Fig. 18). By increasing the applied force, it appears a shear of the upper skin near the impacted area as well as cork cracks (Fig. 17a) and/or cork grain failure (Fig. 17b and c). This damage scenario can be easily adopted for dynamic loading such as impact test.

## 4. Conclusion

The experimental characterisation of impact behaviour by falling mass and quasi-static indentation of a new jute/epoxy-cork sandwich materials has been undertaken. The results show that the cork density and the impact energy affect noticeably the depth damage, the force responsible of the first damage, $F_0$, as well as the maximum force supported by the sandwich panel, $F_{\max}$.

It has been noted that these forces rise with increasing the impact energy and reducing the cork density. When the density increases from 160 to 310 kg/m$^3$, the maximum force recorded decreases of about 60%. This difference can be explained by the fact that, during the manufacturing process by infusion, the resin infiltrates the pores of the agglomerated cork, which leads to increase the material local stiffness.

The sandwich panels manufactured with low density cork are characterised by low elastic behaviour and have a deeper permanent indentation. The increment of the cork density from 160 to

310 kg/m$^3$ leads to a reduction of 3.72% in the energy dissipation capacity when the impact energy is 7 J.

Concerning the damage extent, the decrease in cork density from 310 to 160 kg/m$^3$, generates an 18.43% drop in the permanent indentation depth during the impact tests. This depth drop is always found for the indentation tests, but its extent was reduced to 5.12%.

By comparing the impact test results to those of indentation, it can be concluded that:

- The maximum forces applied on the jute/epoxy-cork sandwich composites, during impact tests, are superior to those of indentation ones.
- This sandwich material type has an energy dissipation capacity, under impact loading, higher than the indentation loading.
- The permanent indentations generated by the quasi-static indentation are deeper than those created by falling weight impact.

## References


[1] Mir A, Zitoune R, Collombet F, Bezzazi B. Study of mechanical and thermo-mechanical properties of jute/epoxy composite laminate. J Reinf Plast Compos 2010;29:1669–80.

[2] Gassan J, Bledzki AK. Effect of moisture content on the properties of silanized jute-composites. Polym Compos 1997;18:179–84.

[3] Mukhopadhyay S, Fangueiro R. Physical modification of natural fibers and thermoplastic films for composites – a review. J Thermoplast Compos mater 2009;22:135–62.

[4] Karmaker AC. Effect of water absorption on dimensional stability and impact energy of jute fibre reinforced polypropylene. J Mater Sci Lett 1997;16:462–4.

[5] Akil HM, Cheng LW, Mohd Ishak ZA, Abu Bakar A, Abd Rahman MA. Water absorption study on pultruded jute fibre reinforced unsaturated polyester composites. Compos Sci Technol 2009;69:1942–8.

[6] Rahman R, Hasan M, Huque M, Islam N. Physico-mechanical properties of jute fiber reinforced polypropylene composites. J Reinf Plast Compos 2010;29(3):445–55.

[7] Khan RA, Khan MA, Zaman HU, Pervin S, Khan N, Sultana S, et al. Comparative studies of mechanical and interfacial properties between jute and E-glass fiber-reinforced polypropylene composites. J Reinf Plast Compos 2010;29(7):1078–88.

[8] Bledzki AK, Mamun AA, Faruk O. Abaca fibre reinforced PP composites and comparison with jute and flax fibre PP composites. eXPRESS. Polym Lett 2007;1(11):755–62.

[9] Santulli C, Caruso AP. A comparative study on falling weight impact of jute/epoxy and hemp/epoxy laminates. Malaysian Polym J 2009;4(1):19–29.

[10] Ray D, Sarkar BK, Rana AK. Fracture behavior of vinylester resin matrix composites reinforced with alkali-treated jute fibers. J Appl Polym Sci 2002;85:2588–93.

[11] O'Dell JL. Natural fibers in resin transfer molded composites. In: Forth woodfiber–plastic composites international conference. Madison, USA; 1997. p. 280–5.

[12] Rashed HMMA, Islam MA, Rizvi FB. Effects of process parameters on tensile strength of jute fiber reinforced thermoplastic composites. J Naval Architec Mar Eng 2006;3:1–6.

[13] Plackett D, Andersen TL, Pedersen WB, Nielsen L. Biodegradable composites based on L-polylactide and jute fibres. Compos Sci Technol 2003; 3: 1287–96.

[14] Sabeel Ahmed K, Vijayarangan S, Kumar A. Low velocity impact damage characterization of woven jute–glass fabric reinforced isothalic polyester hybrid composites. J Reinf Plast Compos 2007; 26: 959–76.

[15] Santulli C. Post-impact flexural tests on jute/polyester laminates monitored by acoustic emission. J Mat Sci 2006;41:1255–9.

[16] Briotti G, Scarponi C, Caneva C, Valente M. New technique for the evaluation of delaminations on low-cost natural fibers composite LAMINATES. In: Fifteenth WCNDT. Roma, Italy; 2000.

[17] Santulli C, Cantwell WJ. Impact damage characterization on jute reinforced composites. J Mat Sci Lett 2001;20:477–9.

[18] Reis L, Silva A. Mechanical behavior of sandwich structures using natural cork agglomerates as core materials. J Sand Struct Mater 2009;11(6):487–500.

[19] Mir A. Etude du comportement mécanique en fatigue des composites stratifié et sandwich à base de renfort en fibres naturelles. Thèse de Doctorat. Université de Boumerdès-Algérie; 2010.

[20] Castro O, Silva JM, Devezas T, Silva A, Gil L. Cork agglomerates as an ideal core material in lightweight structures. Mater Des 2010;31:425–32.

[21] Petit S, Bouvet C, Bergerot A, Barrau JJ. Impact and compression after impact experimental study of a composite laminate with a cork thermal shield. Compos Sci Technol 2007;67:3286–99.

[22] Pereira H, Garcia J, Baptista C. The effect of growth rate on the structure and compressive properties of cork. IAWA Bulletin 1992;13:389–96.

[23] Moussady S, Abdul-Wahab M, Moubayed N, Davies P. Etude du comportement dynamique de panneaux sandwichs à l'impact. In: Annals of the University of Craiova. Electrical Engineering series; 2009. vol. 33. p. 148–53.